The Effect of Electrode Configuration and Substrate Material on the Mass Deposition Rate of Electrospinning

Jonathan Stanger,[1] Nick Tucker,[1] Andrew Wallace,[1] Nigel Larsen,[1] Mark Staiger,[2] Roger Reeves[3]

[1]*New Zealand Institute for Plant and Food Research, Christchurch, New Zealand*
[2]*Department of Mechanical Engineering, University of Canterbury, Christchurch, New Zealand*
[3]*Department of Physics and Astronomy, University of Canterbury, Christchurch, New Zealand*

Received 3 April 2008; accepted 9 November 2008
DOI 10.1002/app.29663
Published online 10 February 2009 in Wiley InterScience (www.interscience.wiley.com).

ABSTRACT: Poly(vinyl alcohol) (PVOH) was electrospun using different methods to charge the polymer solution. A positive high voltage relative to the collecting electrode significantly increased the fiber deposition rate. Electron microscopy showed that approximately half of the increase in fiber mass was due to thicker fibers being deposited. The current flowing from the grounded electrode was measured to determine the charge carried on the PVOH jet. This showed that for a positive voltage charging condition there is a much larger current and hence more charge carriers generated in the PVOH solution. As a result, more mass is ejected from the Taylor cone, implying that a positive voltage also produces longer fiber for a given time period. We also tested whether different substrate materials caused any variation when the charging conditions were changed. Statistically significant variation between substrates was only found when the substrate was an insulator and was expected to support a high-deposition rate. This confirms the view that the PVOH fiber arrives at the collecting electrode carrying a charge that must be neutralized, otherwise a repulsive charge will form where the fiber is deposited and some fiber will be lost to any alternative earth. In electrospraying, charge carriers are generated using associated redox reactions. Thus, for electrospinning a lack of symmetry in these reactions may result in the generation of different quantities of charge carriers in the PVOH solution and changes in the mass deposition rate of electrospun fiber. J Appl Polym Sci 112: 1729–1737, 2009

Key words: electrospinning; polarity; substrate; deposition rate; PVOH; charge carriers

INTRODUCTION

Electrospinning is a low capital way of making nanoscale fibers, defined as having a critical dimension in the nanometer range.[1] Electrospinning uses an electrostatic force to draw fiber from a bead of polymeric fluid.[2] While the fiber is in flight it experiences a bending instability[3,4] leading to a high draw ratio.[5] Draw ratio is the ratio of the initial fiber diameter to the final fiber diameter.

The electrostatic force that drives electrospinning was first observed by Gilbert,[6] but it took some 300 years before the implication of Gilbert's observation gave rise to serious quantitative research. The first work on modeling the process followed from Zeleny's[7] examination of fluid drop behavior under the influence of high strength electrostatic fields. This was extended by Taylor[2,8,9] in his analytical treatment of the eponymous cone. Later developments[4,10–12] used a finite element approach to quantify the bending instabilities experienced by the fiber in flight.

Cooley[13] and Formhals[14] made unsuccessful early attempts at commercialization of the electrospinning process. In the past two decades, the technique was rediscovered as a comparatively simple way to produce small quantities of ultra-fine fibers. For an extended discussion of different methods of producing ultra-fine fibers refer to An Introduction to Electrospinning and Nanofibers.[1] Generally, the low mass deposition rate limits the possible range of applications to niche markets. Consequently, only a small number of companies currently use electrospinning commercially, for example in specialist filtration elements and wound dressings or electrospinning equipment.*

Compared with traditional macroscale fiber production techniques, electrospinning has several advantages. Electrospun fibers can be made with diameters <100 nm in a continuous process.[15] It has also been observed that the draw ratios of the fibers are very large.[5] The high draw ratio can induce increased crystallinity in the resulting fiber.[16] Hence, fibers produced via this method are expected to

Correspondence to: N. Tucker (tuckern@crop.cri.nz).
Contract grant sponsors: New Zealand Institute Crop and Food Research, New Zealand Foundation for Research, Science and Technology via the Technology in Industry Fellowship programme.

*Example companies include Donaldson Filtration Solutions, eSpin Technologies, Electrospinz, and NICAST.

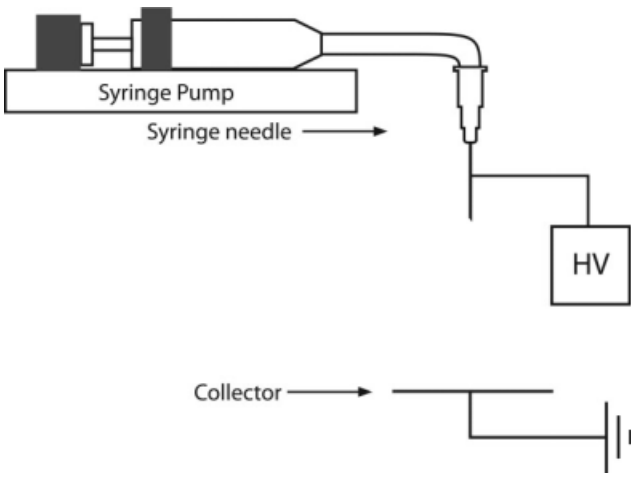

Figure 1 Schematic of essential elements to a typical electrospinning apparatus.

have a tensile strength approaching their theoretical maximum. The high surface area to volume ratio of electrospun materials can be used for medical dressings, drug delivery and active filtration.[17,18]

The arrangement of research electrospinning apparatus is typically a horizontal syringe pump with a needle held at high voltage in proximity to an earthed electrode (the collector).[1] The apparatus provides a simple route to the production of small quantities of fiber (see Fig. 1).

The main process parameters that affect electrospinning[19] are summarized in Table I. Studies have been made of solution properties,[19–24] process parameters[16,21,25–27] and ambient properties.[19,28] A significant challenge in the study of electrospinning is the interdependent nature of the processing parameters. The large number of interacting parameters makes it difficult to combine existing research for the development of large scale, commercial electrospinning techniques.

We observed that when the charging conditions were reversed (i.e., high voltage was moved from needle to collector) there was a significant decrease in the deposition rate of fiber. Originally, it was expected that the change in charging conditions would only result in the change of the sign of the charge on the two electrodes and hence have no effect on the deposition rate. This article reports on our observation of the decrease in deposition and an examination of the cause. We also demonstrate a simple method of optimization for single jet operation using electrostatics and for the optimization of larger multiple jet operations.

EXPERIMENTAL

Electrode configuration

The primary independent variable being examined in all experiments was the electrode configuration. This refers to changing the method of inducing charge on the electrodes used in the electrospinning process. Two electrode configuration pairs were used in our experiments. The first pair used a positive high-voltage power supply to charge the collector electrode and a connection to ground to charge the polymer solution. This was compared with using a positive high voltage to charge the polymer solution and a connection to ground to charge the collector. The second pair used a negative high-voltage power supply to charge the polymer solution and a connection to ground to charge the collector electrode. This was compared with a positive high voltage to charge the polymer solution and a connection to ground to charge the collector electrode. These different electrode configurations are summarized in Table III and Figure 2.

Substrate variation

A secondary independent variable also examined in some of our experiments was the effect of different substrate materials placed over the copper collector electrode on the collection of electrospun fibers. We used a range of substrates with different dielectric constants and conductivities. The relevant properties for the substrate materials used are summarized in Table IV.[29]

Dependent variables

The primary dependent variable measured was the mass deposition rate. This was taken to be the raw

TABLE I
Processing Parameters that Affect the Electrospinning Process

Solution properties	Process parameters	Ambient properties
Concentration	Electrostatic potential	Temperature
Viscosity	Electric field strength	Humidity
Surface tension	Electrostatic field shape	Local atmosphere flow
Conductivity dielectric	Working distance	Atmospheric composition
Constant solvent	Feed rate	Pressure
Volatility	Orifice diameter	

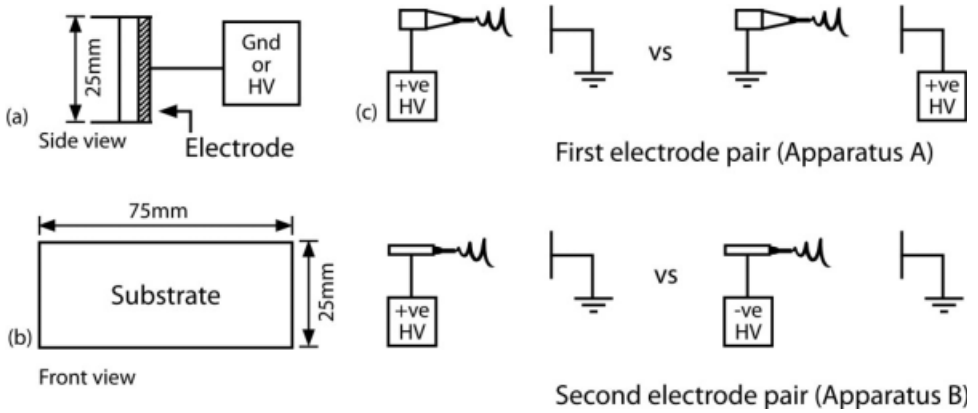

Figure 2 (a) Substrate positioning, (b) Substrate dimensions, and (c) Electrode configurations used.

mass of fiber deposited on a substrate per hour. Each mass deposition rate was calculated from the weight change of the substrates used. This was measured using a Mettler-Toledo AG204 balance reading to 0.0001 g.

One secondary dependent variable measured was the current flow in the electrospinning fiber. This was taken to be the current flowing between ground and the electrode connected to ground. Current measurements were obtained using a Keithley Instruments 610B Electrometer (Cleveland, OH). The Electrometer was placed in series with the grounded electrode when measuring the current flow to protect it from high voltages.

Another secondary dependant variable measured was the fiber diameter. This was calculated using image analysis software applied to images produced by a Field Emission Electron Microscope. The electron microscope used was a JEOL JSM-7000F (Jeol, Tokyo, Japan) field emission scanning electron microscope (FESEM). FESEM micrographs were taken with a voltage of 2 kV to prevent residual charge building up on the polymeric fibers. Each sample of fiber was taken from a 10-s deposition. When gold sputtering was performed the short deposition time allowed for a thin fiber mat which ensured a uniform gold coating.

The final secondary dependent variable measured was the initial jet diameter. This was measured using an optical USB microscope model QX5 (Digital Blue, GA) operating at 60× zoom and calibrated using a standard calibration slide.

Apparatus

Apparatus A

The apparatus used was an Adam series electrospinning apparatus (Electrospinz, Blenheim, New Zealand) (see Fig. 3). This apparatus used the typical electrospinning arrangement of two electrodes, one acting as a collector and the other in contact with the polymer solution. The two electrodes were mounted in a horizontal arrangement on a linear rail and aligned such that their centers shared a common axis. The collector electrode was a copper plate 25 × 25 mm^2 which substrates could be placed over. The spinning tip was an Axygen T-200-Y 200 μL pipette tip with an orifice diameter of 0.8 mm and a copper tube 30-mm long and 3-mm diameter placed in line with the pipette tip to charge the polymer solution. A stable spinning jet was maintained by controlling solution pressure at the spinning tip by raising or lowering the height of the solution header tank whilst observing the needle with the USB microscope (model QX5, Digital Blue).

Apparatus B

This apparatus used a variation on the typical electrospinning arrangement, via a parallel plate

Figure 3 Photograph of Electrospinz Adam Series electrospinning apparatus (microscope not shown for clarity).

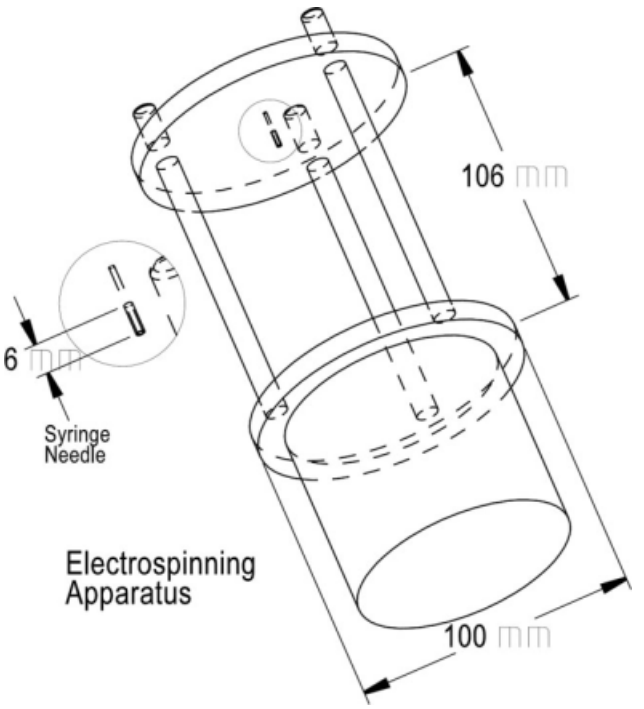

Figure 4 Schematic of apparatus B shown with an isometric tilt to demonstrate detail.

arrangement with one plate as a collector and the other plate charging the polymer solution as it flowed through to the metal spinning tip (a 21-gauge syringe needle) (see Fig. 4). Both parallel plates acting as the electrodes were circular disks of aluminum with a diameter of 100 mm and a thickness of 8 mm. These plates were mounted using three acetyl rods placed every 120° around the edge of the plates ensuring a common axis at the centre of the electrodes. The polymer was charged using an EW series high-voltage power supply (Glassman High Voltage). The polymer solution flow rate was controlled with a KD Scientific model 100 syringe pump.

Solution properties

The polymer used in this work was poly(vinyl alcohol) (PVOH) purchased from BDH Chemicals (VWR International) ID# 297914D. The polymer has a molecular weight of ~115,000 g mol^{-1} and an 87% minimum degree of hydrolysis (DH). The polymer was dissolved in distilled water at an average concentration of 9.66×10^{-4} mol L^{-1}, taking 2 h at 80°C with constant stirring. A dilution of 4.58×10^{-4} mol L^{-1} was used in the following experiments. The density of the final solution was measured to be 1013 kg m^{-3} using a Metler-Toledo XS105 microbalance with specialist density measuring kit. The conductivity of the final solution was measured to be 365 μS using the conductivity meter described by.[30] The dielectric property of the solution is assumed to be the same as the solvent, i.e., $\varepsilon = 78.4$. A series of possible redox reactions that might occur at the spinning head have been summarized in Table II.

TABLE II
Redox Reactions that Might be Possible at the Spinning Head and the Associated Potentials Including those Adjusted for Approximate Solution Ion Concentration

	E_0 (V)
Positively charged solution	
$Cu \rightarrow Cu^{2+} + 2e^-$	−0.34
$4OH^- \rightarrow O_2 + 2H_2O + 4e^-$	−0.40
$[OH^-] = 10^{-8}$ (mol L^{-1})	−0.87
$2H_2O \rightarrow O_2 + 4H^+ + 4e^-$	−1.23
$[H^+] = 10^{-6}$ (mol L^{-1})	−0.88
Negatively charged solution	
$2H^+ + 2e^- \rightarrow H_2$	0.00
$[H^+] = 10^{-6}$ (mol L^{-1})	−0.35
$2H_2O + 2e^- \rightarrow H_2 + 2OH^-$	−0.83
$[OH^-] = 10^{-8}$ (mol L^{-1})	−0.34

Experimental methods

Experiment 1

This experiment examined the mass deposition rate as a function of the substrate material and electrode configuration. Each substrate was cut to 25×75 mm^2. The three substrates examined were standard glass microscope slides, sheets of 100 type N (phosphor doped) silicon wafer and 0.8-mm thick steel. The first pair of electrode configurations was used (Table III and Fig. 2).

The production of fiber was done on apparatus A. The substrate was 50 mm from the pipette tip. The high-voltage power supply was set to deliver 11.5 kV. At this voltage the electrode configuration could be changed and still supply a stable spinning environment without having to alter the supply voltage. For each combination of substrate material and electrode configuration, two samples were produced by depositing fiber for 10 min. From these samples the mass deposition rate was measured and averaged to give one value for each combination of substrate material and electrode configuration.

TABLE III
Summary of the Different Electrode Configurations Used in this Article

	Collector electrode	Polymer solution
"First pair"	Positive high voltage (+ve)	Ground (Gnd)
	Ground (Gnd)	Positive high voltage (+ve)
"Second pair"	Ground (Gnd)	Negative high voltage (−ve)
	Ground (Gnd)	Positive high voltage (+ve)

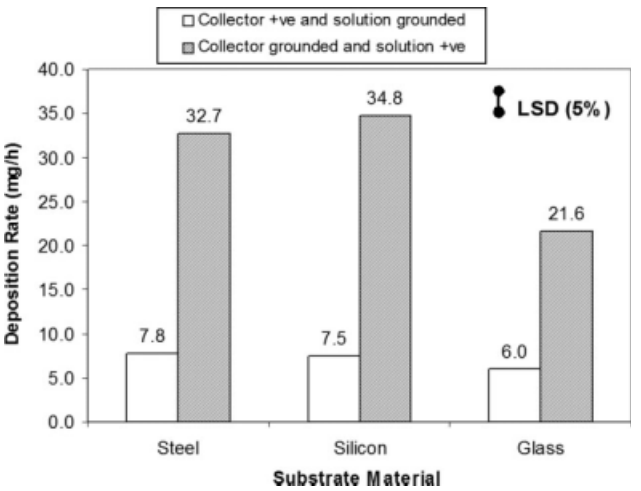

Figure 5 Average mass deposition rates measured for experiment 1. Differences between means are statistically significant at the 5% level if they exceed the LSD(5%).

Experiment 2

This experiment measured the fiber diameter, initial jet diameter and the current flow as a function of the electrode configuration. Fiber samples were produced by depositing for 10 s onto an aluminum foil substrate. The electrode configurations used were the first pair (Table III and Fig. 2). After these samples were obtained the deposition was continued and the initial jet diameter and current flow was measured. The initial jet diameter was measured as described in the dependent variables section. The current flow was measured between a ground source and the electrode connected to ground in the method described in the dependent variables section.

The production of fiber was done on apparatus A. The substrate was 50 mm from the pipette tip. The high-voltage power supply was set to deliver 11.5 kV. At this voltage the electrode configuration could be changed and still supply a stable spinning environment without having to alter the supply voltage.

Experiment 3

This experiment measured the mass deposition rate as a function of the electrode configuration. The electrode configurations used were the second pair (Table III and Fig. 2). For the electrode configuration collector (Gnd)/solution (−ve) five samples of fiber were collected. For each electrode configuration collector (Gnd)/solution (+ve) seven samples of fiber were collected. Each sample was the result of 10 min of deposition.

Apparatus B was used to produce the fiber. The substrate used was aluminum foil of dimensions 60 × 60 mm^2. The substrate was 100 mm from the needle tip. When the polymer solution electrode was charged to a negative potential the flow rate required for a stable Taylor cone was 0.32 mL h^{-1}, whereas, when the electrode was charged to a positive potential the flow rate required was 0.62 mL h^{-1}. The high-voltage power supply was set to deliver 33 kV. At this voltage, stable spinning could be obtained for both electrode configurations.

ANALYSIS AND DISCUSSION OF RESULTS

Experiment 1

This experiment served as an initial examination of possible substrate effects on the deposition rate (Fig. 5). The chosen substrates covered both a range of dielectric constants and conductivities (Table IV). The results presented in Table V and Figure 5 were obtained by performing an ANOVA for two factors (substrate and electrode configuration) with repeats on the raw data for experiment 1. Differences between treatments were compared with the Least Significant Difference (LSD) calculated for the 5% level of significance. This has the property that differences between treatment means are statistically significant at the 5% level if they exceed the LSD(5%).[31] These results demonstrate that the electrode configuration is the primary source of variation P (0.001), with steel and silicon collectors in the collector (Gnd)/solution (+ve) configuration depositing at an average of 4.4 times the rate of the collector (+ve)/solution (Gnd) configuration. However both the substrate ($P = 0.005$) and the interaction between factors ($P = 0.018$) are also statistically significant sources of variation. Figure 5 shows that glass with a configuration of collector (Gnd)/solution (+ve) has

TABLE IV
Physical Properties of the Substrate Materials

Material	Dielectric constant	Conductivity
Aluminum	∞	3.6×10^{7}
Steel	∞	1×10^{7}
Silicon	11.5	1.6×10^{-3}
Glass	3.8	1×10^{-12}

TABLE V
Values of the Dependent Variable Measured in Experiment 2

Electrode configuration	Initial jet diameter (m)	Fiber diameter (m)	Current flow (μA)
Collector (+ve) Solution (Gnd)	1.22×10^{-5}	1.7×10^{-7}	0.30
Collector (Gnd) Solution (+ve)	3.52×10^{-5}	2.8×10^{-7}	0.85

TABLE VI
ANOVA Results for the Raw Data in Experiment 1

Source of variation	Degrees of freedom	Mean squares	Variance ratio	*F* probability
Substrate	2	6.43×10^{-5}	14.29	0.005
Electrode configuration	1	1.53×10^{-3}	340.00	<0.001
Interaction between factors	2	3.82×10^{-5}	8.49	0.018
Residual	6	4.50×10^{-6}		
Total	11			

a deposition rate only about two thirds of the rate with silicon and steel substrates (12 mg h^{-1} less, *P* (0.05), whereas the deposition rates with collector (+ve)/solution (Gnd) are similar across the 3 substrates ($P > 0.05$). Thus, the differential response to glass when the polarity of the electrodes is reversed is the main source of the variation due to interaction. The physical cause of this variation is that, when the larger mass throughput is required, the low conductivity of the glass becomes a significant limiting factor. Hence, the charge flow across the substrate is being limited, allowing the charge on incoming fiber to build up and repel new fiber.

Experiment 2

Using the average fiber diameter measured from images such as Figure 6 (see Table VI) it is possible to use eq. (1) (below) to calculate the factor by which the volume changes for the deposited fiber onto an aluminum collector when the electrode configuration is changed. The increase in volume of fiber produced using an electrode configuration of collector (Gnd)/solution (+ve) is a factor of 2.7 times the volume obtained by using a configuration of collector (+ve)/solution (Gnd). This is compared to an increase in mass deposition rate by a factor of over 4 for the same electrode configurations using steel and silicon substrates.

$$V = \pi r^2 l \tag{1}$$

where *V* is the volume of fiber (m^3), r is the average radius of fiber (m), and l is the length of fiber (m).

The results from Table V allow the calculation of further parameters describing the state while electrospinning is active. Equations 2 and 3 can be solved to give the total velocity of the fiber while in flight. These equations are modified from.[5] Note that this velocity is the length of the vector summation of both the tangential "whipping" velocity and the parallel velocity of fiber traveling toward the collector. Additionally using the velocity in eqs. (3) and (4) can be solved to give the charge per unit length when the fiber contacts the substrate. These values are summarized in Table VII.

$$v_1 = \frac{w_1}{\rho_1 \pi r_1^2 t_1} \tag{2}$$

where v_1 is the velocity of the aqueous jet (ms^{-1}), w_1 is the weight of solution used (kg), ρ_1 is the density

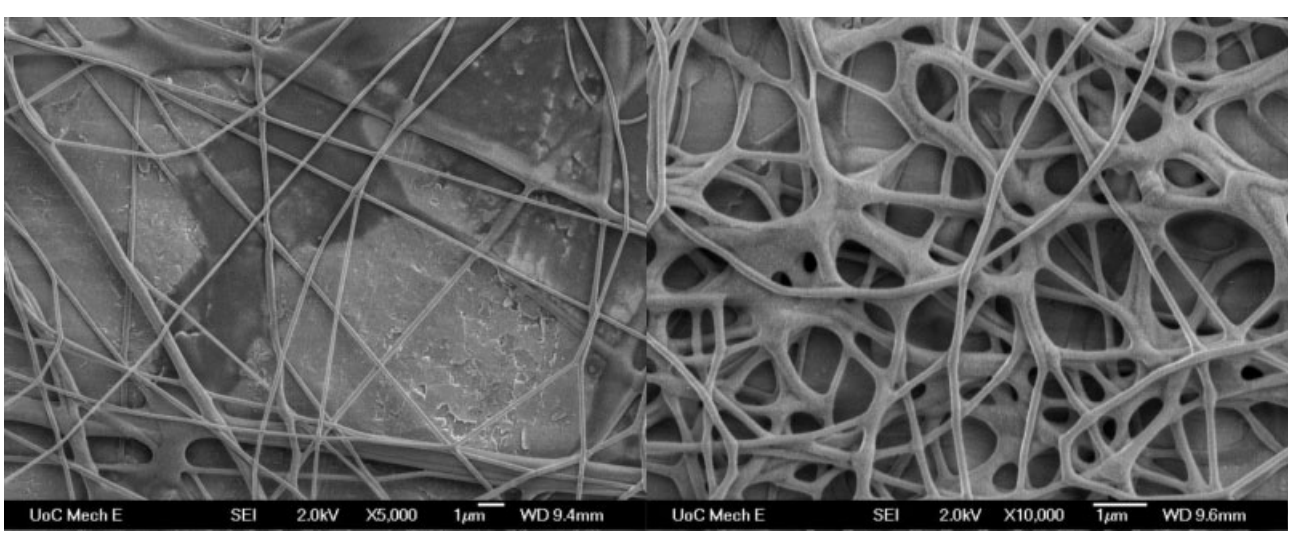

Figure 6 Example FESEM images used to measure the final fiber diameter.

TABLE VII
Summary of Results from Equations (2), (3), and (4)

Electrode configuration	Initial velocity of fluid in jet v_1 (ms^{-1})	Velocity of fiber at substrate v_2 (ms^{-1})	Charge per unit length σ (Cm^{-1})
Collector (+ve) Solution (Gnd)	0.30	63	4.75×10^{-9}
Collector (Gnd) Solution (+ve)	0.20	130	6.56×10^{-9}

of the polymer solution (measured to be 1013 kg m^{-3}), r_1 is the radius of the polymer jet (m), and t_1 is the time spent spinning the fiber (s).

$$v_2 = \frac{w_2}{\rho_2 \pi r_2^2 t_2} \tag{3}$$

where v_2 is the spinning velocity when the fiber hits the substrate (ms^{-1}), w_2 is the weight of the fiber on the substrate (kg), ρ_2 is the density of the spun fiber (1260 kg m^{-3}), r_2 is the radius of the spun fiber (m), and t_2 is the time spent spinning the fiber (s).

$$\sigma = \frac{I}{v_2} \tag{4}$$

where I is the current flow in the circuit formed by the electrospinning apparatus (A), v_2 is the velocity when the fiber hits the substrate (ms^{-1}) and σ is the charge per unit length on the fiber as it hits the substrate (cm^{-1}).

Experiment 3

One objection to the results obtained so far is that they have used the ground as the source of negative charge. As the ground is not a true negative charge source the experiment was repeated using a convertible power supply so that the effects of a negative charge can be directly compared to a positive charge. The positive charge solution deposited at 35 mg h^{-1} compared to 16.4 mg h^{-1} with the negatively charged solution. Performing ANOVA on the raw data showed that the variance due to charge polarity is significantly larger than the variance of the data and hence there is a significant effect due to the charge polarity used on the polymer solution.

Substrate effects

Analysis of experiment 1 reveals that not all substrates share the same behavior. Figure 5 shows that using glass substrates will result in a significant decrease in the mass deposition rate. It is proposed that the conductivity of the glass substrate is low enough to hinder the neutralization of the charges on incoming fiber. This would result in a build-up of a charge on the substrate that would repel the incoming fiber similarly to that proposed by.[32] Silicon, however, has a high enough conductivity to perform and the metals. Hence, it is proposed that if a substrate material has a conductivity below a critical value then the deposition rate of fiber in electrospinning will decrease. This critical value, however, will depend on the charge density on the fiber and the mass deposition rate and hence will be different for almost all electrospinning conditions. A detailed exploration of the exact critical value has not been undertaken in this work.

Effect on deposition rate

The results of these experiments clearly show that as the electrode configuration is changed there is a change in mass deposition rate. Application of a positive high voltage to the polymer solution must generate a positive charge on the solution. In all experiments, this results in a higher deposition rate. Application of a negative high voltage to the solution in experiment 3 has similar results to the application of ground to the solution in experiment 1, where a metallic substrate was also used. The application of ground in these cases must be acting to generate a negative charge to counter the positive charge generated by the high-voltage power supply. With all other factors held equal, changing the charge polarity should simply result in the reversal of the electric field direction. However, the reversal of the electric field direction should have no effect on the mass deposition rate. Hence, as shown in experiment 2 there must be a different quantity of charge being generated, depending on the charge polarity. This would result in a difference in the forces being exerted on the polymer solution and hence the difference in the mass deposition rate.

It should be noted, however, that the results from experiment 3 cannot be directly compared with the results of the other two experiments as ground cannot act as a perfect negative supply. Unless the grounded electrode is essentially the only object that can act as ground in an effective infinite space then other ground sources will also generate a negative charge. This charge is proportional to the distance from the high-voltage electrode and as such in an apparatus as described in this article would be small. However, even a small charge will reduce the efficiency of the grounded electrode acting as a negative supply. Because of this low efficiency, the results in the first two experiments will be partly due to a change in the electrostatic field between the

two electrodes. Hence, direct comparison between the results of the two different electrode configuration pairs is unsound; however, the trend is still obvious in all experiments. Further discussion of the electric field effects on the mass deposition rate are beyond the scope of this article.

Examination of literature relating to electrospraying,[33–35] a process related to electrospinning, shows that these processes can be viewed as a simple redox cell.[34] A redox reaction typically consists of a pair of reactions, a reduction involving a species gaining an electron and an oxidation involving a species losing an electron.[36] This is driven either by the energetic favorability of the products or by forcing a current to flow through the solution. Electrospraying and electrospinning are electric current driven processes. At the positively charged electrode, an oxidation reaction occurs and conversely at a negatively charged electrode a reduction reaction occurs. This results in a net flow of charged species, completing the electrical circuit. In this treatment there is no free surface charge, all charge is carried by the species generated in the redox reactions.

If there was a lack of symmetry in the redox reactions that occur, then dependent on the polarity of the charging electrode there would be a different quantity of charge carriers produced. This change in the quantity of charge carriers would be mirrored in the mass deposition rate because the charge determines the force on the solution. If there was a higher charge generated for one of the charge carrier polarities then it is expected that there would be a significant difference in the velocity that the fiber would reach in flight.

Therefore, it is proposed that the change in the mass deposition rate is due to a higher capacity for positive charge carriers to be generated than negative charge carriers in a PVOH solution. Experiment 2 shows that there is a significantly higher final velocity when a positive charge is used, which is expected from eq. 5 below[37] if a higher charge is generated. The initial velocity of the fluid jet also supports this claim as the conditions where there is a higher charge should result in a larger mass being expelled from the Taylor cone.[2] As the larger mass has had little time to take advantage of its higher charge and accelerate in the electrostatic field it should have a slower speed. Furthermore, it is well known that like charges repel[37] and as such during the jet thinning process if the jet held a higher concentration of charge the final fiber will be thicker. This is due to the charge on the jet forcing the surface outward, countering the jet thinning. The draw ratio of the fiber in question also shows that the generation of a positive charge results in less jet thinning. Finally, the current measurements in experiment 2 directly show the higher charge when a positive source is used to charge the polymer solution.

$$F = Eq \tag{5}$$

where F is the force experienced by a charged object (N), E is the electric field (V/m) and q is the charge on the object (C).

These conclusions reflect the same conclusions reached by previous authors[38–40] using polyamide-6 or polyacrylonitrile. However, here this discussion links the observed differences to the generation of charged species *in situ* (as accepted in electrospraying[34]) rather than charged species generated in the solution preparation.

CONCLUSION

The substrate material has no effect on the mass deposition rate in an electrospinning process unless the material's conductivity is below a critical value. Insulating materials will allow a repulsive charge to build up on the substrate, decreasing the mass deposition rate.

The generation of a positive charge in a solution of water and PVOH with a copper electrode results in a higher quantity of charge carriers than the negative case. The generation of charge carriers is explained using work done on the analogous process of electrospraying. The higher quantity of charge carriers causes a lower draw ratio and thicker fibers but a larger quantity of fiber is produced and a higher final speed upon deposition.

The authors thank the University of Canterbury for their help with equipment; particularly Mike Flaws for his assistance with the FESEM and Electrospinz Ltd, 44 Lee St, Blenheim, New Zealand (www.electrospinz.co.nz) who supplied the electrospinning machine.

References

1. Ramakrishna, S.; Fujihara, K.; Teo, W.; Lim, T.; Ma, Z. An Introduction to Electrospinning and Nanofibers; World Scientific: Singapore, 2006.
2. Taylor, G. Proc R Soc London Ser A 1969, 313, 453.
3. Reneker, D. H.; Yarin, A. L.; Fong, H.; Koombhongse, S. J Appl Phys 2000, 87, 4531.
4. Yarin, A. L.; Koombhongse, S.; Reneker, D. H. J Appl Phys 2001, 89, 3018.
5. Wang, H.; Shao, H.; Hu, X. J Appl Polym Sci 2005, 101, 961.
6. Gilbert, W. De Magnete, Magneticisque Corporibus, et de Magno Magnete Tellure (On the Magnet and Magnetic Bodies, and on That Great Magnet the Earth); Peter Short: London, 1628.
7. Zeleny, J. Phys Rev 1914, 3, 69.
8. Taylor, G. Proc R Soc London Ser A 1964, 280, 383.
9. Taylor, G. Proc R Soc London Ser A 1965, 291, 145.
10. Hohman, M. M.; Shin, M.; Rutledge, G.; Brenner, M. P. Phys Fluids 2001, 13, 2201.

11. Hohman, M. M.; Shin, M.; Rutledge, G.; Brenner, M. P. Phys Fluids 2001, 13, 2221.
12. Yarin, A. L.; Koombhongse, S.; Reneker, D. H. J Appl Phys 2001, 90, 4836.
13. Cooley, J. F. U.S. Pat. 692,631 (1902).
14. Formhals, A. U.S. Pat. 1,975,504, (1934).
15. Sundaray, B.; Subramanian, V.; Natarajan, T. S.; Xiang, R.-Z.; Chang, C.-C.; Fann, W.-S. Appl Phys Lett 2004, 84, 1222.
16. Zhao, S.; Wu, X.; Wang, L.; Huan, G. Y. J Appl Polym Sci 2004, 91, 242.
17. Shanmugasundaram, S.; Griswold, K. A.; Prestigiacomo, C. J.; Arinzeh, T.; Jaffe, M. Applications of Electrospinning: Tissue Engineering Scaffolds and Drug Delivery System; New Jersey Institute of Technology: NJ, 2004; p 140–141.
18. Tsai, P. P.; Schreuder-Gibson, H.; Gibson, P. J Electrostatics 2002, 54, 333.
19. Mit-uppatham, C.; Nithitanakul, M.; Supaphol, P. Macromol Chem Phys 2004, 205, 2327.
20. Fong, H.; Chun, I.; Reneker, D. H. Polymer 1999, 40, 4585.
21. Jarusuwannapoom, T.; Hongrojjanawiwat, W.; Jitjaicham, S.; Wannatong, L.; Nithitanakul, M.; Pattamaprom, C.; Koombhongse, P.; Rangkupan, R.; Supaphol, P. Eur Polym J 2005, 41, 409.
22. Shenoy, S. L.; Bates, W. D.; Frisch, H. L.; Wnek, G. E. Polymer 2005, 46, 3372.
23. Wannatong, L.; Sirivat, A.; Supaphol, P. Polym Int 2004, 53, 1851.
24. Zeng, J.; Xu, X.; Chen, X.; Liang, Q.; Bian, X.; Yang, L.; Jing, X. J Controlled Release 2003, 92, 227.
25. Deitzel, J. M.; Kleinmeyer, J.; Harris, D.; Beck Tan, N. C. Polymer 2001, 42, 261.
26. Mo, X. M.; Xu, C. Y.; Kotaki, M.; Ramakrishna, S. Biomaterials 2004, 25, 1883.
27. Zhong, X.; Kim, K.; Fang, D.; Ran, S.; Hsiao, B. S.; Chu, B. Polymer 2002, 43, 4403.
28. Casper, C. L.; Stephens, J. S.; Tassi, N. G.; Chase, D. B.; Rabolt, J. F. Macromolecules 2004, 37, 573.
29. CRC. In Handbook of Chemistry and Physics; Lide, L. R., Ed.; CRC Press: Cleveland, OH, 2004.
30. da Rocha, R. T.; Gutz, I. G. R.; do Lago, C. L. J Chem Educ 1997, 74, 572.
31. Snedecor, G. W.; Cochran, W. G. Statistical Methods, 7th ed.; The Iowa State University Press: Ames, Iowa, 1980.
32. Liu, L.; Dzenis, Y. A. Nanotechnology 2008, 19, 355307.
33. Berkel, G. J. V.; Kertesz, V. J Mass Spectrom 2001, 36, 1125.
34. Blades, A. T.; Ikonomou, M. G.; Kebarle, P. Anal Chem 1991, 63, 2109.
35. Wilhelm, O. Electrohydrodynamic Spraying—Transport, Mass and Heat Transfer of Charged Droplets and Their Application to the Deposition of Thin Functional Films. Ph.D Thesis, Swiss Federal Institute of Technology, Zurich, 2004.
36. Chang, R. Chemistry; McGraw Hill: New York, 1998.
37. Halliday, D.; Resnick, R.; Walker, J. Fundamentals of Physics; Wiley: New York, 2001.
38. Mit-uppatham, C.; Nithitanakul, M.; Supaphol, P. Macromol Symp 2004, 216, 293.
39. Supaphol, P.; Mit-uppatham, C.; Nithitanakul, M. Macromol Mater Eng 2005, 290, 933.
40. Sutasinpromprae, J.; Jitjaicham, S.; Nithitanakul, M.; Meechaisue, C.; Supaphol, P. Polym Int 2006, 55, 825.